Hybrid master oscillator power amplifier high-power narrow-linewidth nanosecond laser source at 257 nm

Xavier Delen, Loïc Deyra, Aurélien Benoit, Marc Hanna, François Balembois, Benjamin Cocquelin, Damien Sangla, François Salin, Julien Didierjean, Patrick Georges

Hybrid master oscillator power amplifier high-power narrow-linewidth nanosecond laser source at 257 nm

Xavier Délen,[1,*] Loïc Deyra,[1] Aurélien Benoit,[2,3] Marc Hanna,[1] François Balembois,[1] Benjamin Cocquelin,[2] Damien Sangla,[2] François Salin,[2] Julien Didierjean,[4] and Patrick Georges[1]

[1]*Laboratoire Charles Fabry, Institut d'Optique, CNRS, Univ Paris Sud, 2 avenue Augustin Fresnel, Palaiseau 91127, France*

[2]*Eolite systems, 11 avenue Canteranne, Pessac 33600, France*

[3]*Institut de recherche XLIM, UMR CNRS/Université de Limoges 7252, 123 avenue Albert Thomas, Limoges 87060, France*

[4]*Fibercryst, La Doua, Batiment L'atrium, Boulevard Latarjet, Villeurbanne 69616, France*

**Corresponding author: xavier.delen@institutoptique.fr*

We report on a high-power narrow-linewidth pulsed laser source emitting at a wavelength of 257 nm. The system is based on a master oscillator power amplifier architecture, with Yb-doped fiber preamplifiers, a Yb:YAG single crystal fiber power amplifier used to overcome the Brillouin limitation in glass fiber and nonlinear frequency conversion stages. This particularly versatile architecture allows the generation of Fourier transform-limited 15 ns pulses at 1030 nm with 22 W of average power and a diffraction-limited beam ($M^2 < 1.1$). At a repetition rate of 30 kHz, 106 μJ UV pulses are generated corresponding to an average power of 3.2 W.

There is an increasing need for narrow linewidth, high average power ultraviolet (UV) laser sources for high-resolution spectroscopy, remote environmental sensing, laser-induced fluorescence, semiconductor inspection, and LIDAR applications [1,2]. A standard way of designing efficient sources in the UV is to frequency convert near-infrared diode-pumped solid-state lasers [3,4]. In this case, obtaining high nonlinear conversion efficiency requires a large peak power in the fundamental wave. At a fixed repetition rate and average power, this results in a trade-off between attainable linewidth, related to the pulse duration, and the final nonlinearly converted average power.

Ytterbium-doped fiber amplifiers are particularly attractive to design high power sources at 1030 nm, providing compactness, efficiency, and high beam quality. In narrow linewidth regime (<100 MHz), the physical effect that limits the achievable power is stimulated Brillouin scattering (SBS). The use of large mode area (LMA) fibers and various SBS mitigating techniques has allowed scaling up of the peak power to around 1 kW in a 10 MHz bandwidth [5]. However, this peak power level is still too low for efficient frequency quadrupling to reach the wavelength of 257 nm. In this case, resonant cavities might be used to generate UV light efficiently [6], at the price of an increased complexity.

Recently, single-crystal fiber (SCF) amplifiers have demonstrated a great potential to scale fiber systems beyond their limits fixed by nonlinear effects, while retaining the possibility to generate high average powers [7]. This power scaling has been recently reported in a chirped-pulse femtosecond amplifier [8], allowing the generation of 1 mJ 380 fs pulses with a moderate stretching ratio impossible to attain with glass fibers due to self-phase modulation.

In this Letter, we demonstrate that Yb:YAG SCF amplifiers can be used to scale the power of SBS-limited 15–150 ns pulse ytterbium-doped fiber sources. Subsequent single-pass nonlinear conversion in bulk crystals permits the generation of Fourier transform-limited 15 ns pulses with 3.2 W of average power, or 150 ns pulses with 430 mW of average power at a repetition rate of 30 kHz at 257 nm.

The source is built following a master oscillator power amplifier (MOPA) architecture similar to [9], with an experimental setup depicted in Fig. 1. It starts with a CW single-frequency distributed-feedback (DFB) laser diode emitting 5 mW at 1030 nm with spectral linewidth below 1 MHz. First, this signal is amplified to 50 mW in a single-mode fiber preamplifier with 6 μm core diameter. A fiber-pigtailed acousto-optic modulator (AOM) is then used to carve nanosecond pulses with a variable duration of 15–150 ns at a high repetition rate of 330 kHz in order to limit the amplified spontaneous emission (ASE). This signal is amplified in two stages of single-mode 6 and 15 μm core diameter Yb-doped fiber amplifiers to an average power of 400 mW. A second AOM further decreases the repetition rate to a few tens of kilohertz before coupling to the final LMA fiber amplifier. This amplifier is made of a 2 m long polarizing double-clad 40/200 μm Yb-doped photonic crystal fiber pumped by a 25 W

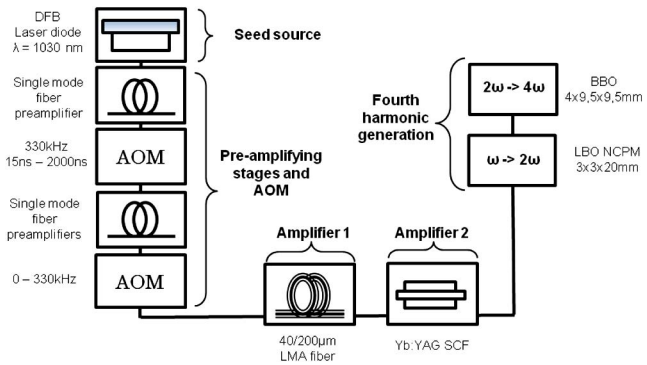

Fig. 1. (Color online) Experimental setup.

fiber-coupled laser diode system at 976 nm. The beam is then further amplified in an Yb:YAG SCF amplifier and converted into UV through a fourth-harmonic generation stage.

To study the SBS threshold in the last fiber amplification stage and characterize the amplified signal, we measured the output spectral linewidth. Part of the CW signal from the DFB diode is sent into a 2 km long optical fiber and used to establish a beating signal with the amplified output after the LMA fiber or the SCF amplification stage. It allows for heterodyne measurement of the narrow linewidth spectrum after different amplification stages [10]. The initial optical frequency is shifted twice by the AOMs through the amplification process. The beating frequency is observed at 90 MHz corresponding to the difference between the two shifts of 110 and 200 MHz of the AOMs. For example, Fig. 2 shows the beating signal and its Fourier transform for 150 ns pulses after the LMA fiber. In this case the linewidth at FWHM is 7 MHz, which is close to the Fourier transform limit.

The final repetition rate is first set to 10 kHz to study the SBS threshold as a function of linewidth at the output of the LMA fiber amplifier. The SBS threshold is detected by looking at the temporal profile of the output pulses, which is distorted when significant SBS occurs. Since the output pulse energy level is over 100 μJ, significant saturation is observed in the fiber amplifier, leading to possible modifications of the temporal profile both in intensity and phase in the time domain, as shown in Fig. 3. (right) The heterodyne measurement is therefore used to measure accurately the optical linewidth for each selected pulse duration. Figure 3 (left) shows that the large

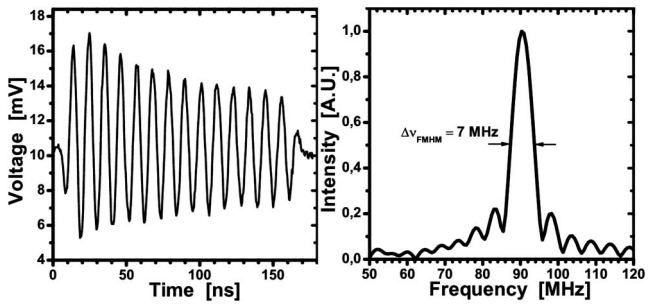

Fig. 2. Left: beating signal obtained after the LMA fiber amplifier for a 150 ns pulse. Right: Fourier transform of the beating signal.

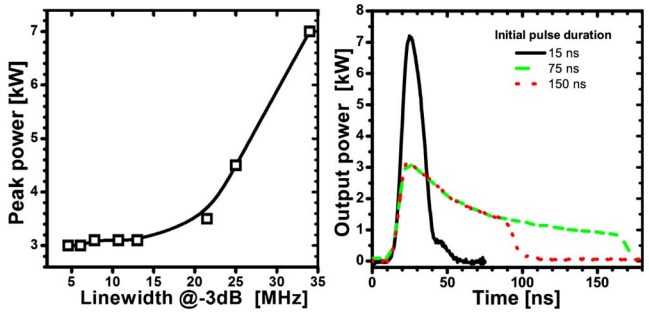

Fig. 3. (Color online) Left: SBS threshold peak power at 10 kHz as a function of the output linewidth in the LMA fiber amplifier. Right: pulse shapes after the LMA fiber amplifier for different initial durations.

core diameter and short length of the fiber power amplifier allow to reach peak powers of 7 kW for 15 ns pulses (35 MHz linewidth at FWHM), with an SBS threshold decreasing to about 3 kW for pulse durations above 75 ns corresponding to linewidth below 13 MHz. Although at the state of the art for narrow linewidth fiber amplifier, the peak powers obtained are not sufficient for efficient frequency-quadrupling.

To further scale the power, an Yb:YAG SCF double-pass amplifier is added at the output of the LMA fiber amplifier. The crystal has an Yb doping concentration of 1 at. %, a diameter of 1 mm, and a length of 4 cm. It is set in a water-cooled mount at 16°C and pumped in single pass by a 75 W high brightness laser diode system at 940 nm coupled to a 105 μm fiber with NA 0.15. The free-propagating signal waist diameter inside the SCF is 400 μm, and the highly multimode pump beam is focused on the same diameter inside the crystal rod. In the SCF, the pulse energy is not limited by SBS but by damage threshold on the AR coated facets, occurring at 5 to 7 J/cm^2 for 500 ps pulses. The repetition rate was therefore adjusted to 30 kHz to remain well below this limit for reliable operation of the system. Figure 4 (left) shows the output power as a function of pump power, for input pulse duration of 15 ns and input average powers ranging from 100 mW to 2.5 W. Between 95% and 97% of the pump power is absorbed by the SCF depending on the seed power. A maximum average power of 22.5 W is reached, corresponding to an optical-to-optical efficiency of 27%, and pulse energy of 750 μJ. It corresponds to a peak power higher than 50 kW, which is seven times higher than the peak power at SBS threshold in glass fiber for this pulse duration.

For 22 W average power, the optical spectrum obtained using an optical spectrum analyzer is displayed in Fig. 4 (right). The spectrum is essentially free of ASE with over 97% of the power in the main peak. Heterodyne linewidth measurements for pulses amplified in the SCF confirm that they remain Fourier-transform-limited, resulting in linewidths of 5–35 MHz at 1030 nm depending on the pulse duration. As shown in Fig. 4 (inset), the beam quality at the output of the SCF is diffraction-limited with $M^2 < 1.1$ in both transverse directions.

Frequency conversion to 257 nm is performed using two successive second-harmonic generation (SHG) stages. The first stage uses a $3 \times 3 \times 20$ mm LBO crystal cut for noncritically phase-matched type I SHG at

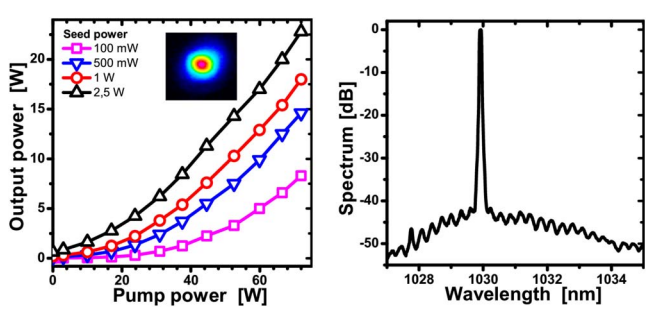

Fig. 4. (Color online) Left: output power as a function of pump power for the SCF amplifier (inset: beam profile at full pump power for a seed power of 2.5 W). Right: optical spectrum at maximum power and pulse width of 150 ns.

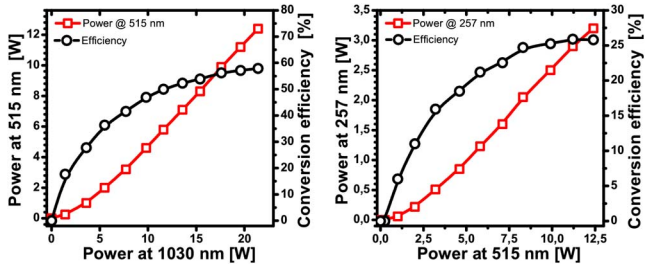

Fig. 5. (Color online) Left: power at 515 nm and conversion efficiency as a function of input power at 1030 nm. Right: power at 257 nm and conversion efficiency as a function of input power at 515 nm. The fundamental pulse duration is 15 ns.

1030 nm. It is AR coated at 1030 and 515 nm, and mounted in an oven at 187.8°C. The amplified beam is focused on a diameter of 120 μm inside the crystal. The power obtained at 515 nm and conversion efficiency are plotted as a function of fundamental power in Fig. 5 (left) for a pulse duration of 15 ns. The efficiency reaches 58% for a maximum power of 12.4 W at 515 nm, showing that the peak power is sufficient for efficient frequency conversion. The green beam quality remains excellent, with M^2 values lower than 1.1 in both directions.

The second SHG stage is based on an uncoated $4 \times 9.5 \times 9.5$ mm BBO crystal cut for critically phase-matched type I SHG at 515 nm. No temperature regulation of the crystal was implemented. To maximize the conversion efficiency, we used elliptical focusing down to 40×150 μm waists to remain within the angular acceptance of the crystal. The power obtained at 257 nm and conversion efficiency of the second SHG stage are displayed in Fig. 5 (right). A maximum power of 3.2 W is obtained, an unprecedented value to our knowledge for a single frequency laser at 257 nm without using nonlinear conversion in resonant cavities. Although the UV average power is stable for hours below 2 W, above this level, power instabilities related to absorption and thermal effects in the crystal start to appear. An optimized thermal management of the BBO crystal should allow increasing this 2 W threshold for appearance of thermal instabilities.

To highlight the trade-off between linewidth and available average power, Table 1 summarizes the results obtained for pulse durations ranging from 15 to 150 ns at 1030 nm after amplification. The generated UV power remains above 400 mW in all cases, making this source a versatile tool for LIDAR and remote sensing applications.

In conclusion, we demonstrate the use of a Yb:YAG SCF amplifier to scale the peak power of SBS-limited Yb-doped single-frequency fiber-based MOPA sources. Furthermore, we show subsequent efficient nonlinear conversion to the fourth harmonic at 257 nm. The performance of the presented hybrid source is currently essentially limited by the available pump power and damage thresholds of coatings of the SCF and the LBO crystal. Higher pump power should also allow power scaling to the 50 W level at 1030 nm without any further modification of the system architecture. Frequency conversion efficiencies could also potentially be improved with higher damage thresholds of the coatings. We believe that this type of architecture could be the basis for next generation LIDAR systems in the UV spectral range.

Table 1. Summary of the Hybrid Source Performances for Various Initial Pulse Widths at a Repetition Rate of 30 kHz

Δt (ns)	15	50	100	150
$\Delta\nu$ (MHz)	40	21	11	6.2
Power at 515 nm (W)	12.4	10.4	7.8	6.3
UV power at 257 nm (W)	3.2	1.8	0.85	0.43

The authors acknowledge the DGA for the funding of this project.

References

1. A. T. Case, D. Tan, R. E. Stickel, and J. Mastromarino, Appl. Opt. **45**, 2306 (2006).
2. M. Ostermeyer, P. Kappe, R. Menzel, and V. Wulfmeyer, Appl. Opt. **44**, 582 (2005).
3. M. Laurila, J. Saby, T. T. Alkeskjold, L. Scolari, B. Cocquelin, F. Salin, J. Broeng, and J. Lægsgaard, Opt. Express **19**, 10824 (2011).
4. A. Diening, S. McLean, and A. Starodoumov, Proc. SPIE **7195**, 71950H (2009).
5. Y. Jeong, J. Nilsson, J. K. Sahu, D. N. Payne, R. Horley, L. M. B. Hickey, and P. W. Turner, IEEE J. Sel. Top. Quantum Electron. **13**, 546 (2007).
6. T. Sudmeyer, Y. Imai, H. Masuda, N. Eguchi, M. Saito, and S. Kubota, Opt. Express **16**, 1546 (2008).
7. Y. Zaouter, I. Martial, N. Aubry, J. Didierjean, C. Hönninger, E. Mottay, F. Druon, P. Georges, and F. Balembois, Opt. Lett. **36**, 748 (2011).
8. X. Délen, Y. Zaouter, I. Martial, N. Aubry, J. Didierjean, C. Hönninger, E. Mottay, F. Balembois, and P. Georges, Opt. Lett. **38**, 109 (2013).
9. R. Zhu, J. Wang, J. Zhou, J. Liu, and W. Chen, Appl. Opt. **51**, 3826 (2012).
10. T. Okoshi, K. Kikuchi, and A. Nakayama, Electron. Lett. **16**, 630 (1980).